

Supplement of Atmos. Chem. Phys., 20, 83–98, 2020
<https://doi.org/10.5194/acp-20-83-2020-supplement>
© Author(s) 2020. This work is distributed under
the Creative Commons Attribution 4.0 License.



Supplement of

Regional variability in black carbon and carbon monoxide ratio from long-term observations over East Asia: assessment of representativeness for black carbon (BC) and carbon monoxide (CO) emission inventories

Yongjoo Choi et al.

Correspondence to: Yongjoo Choi (choingjoo@jamstec.go.jp)

The copyright of individual parts of the supplement might differ from the CC BY 4.0 License.

S1 Seasonal variation in dominant emission regions

Figure S2 shows the seasonal variation in data frequency and total mean fraction of dominant emission regions when APT was zero (without precipitation). Depending on the geographical characteristics, there is a distinct pattern of dominant emission regions. We decided that the valid dominant emission regions would only be considered when the fraction of frequency was higher than 5% to ensure an adequate statistical analysis. As a result, Baengnyeong was suitable for monitoring the Chinese regions (East, North, and Northeast; 14–25%) and Korea (South and North; 8.1% and 16%, respectively), whereas Gosan was mainly influenced by the Chinese regions (11–20%) and South Korea (37%), along with a decreasing fraction of North Korea (4.2%). The Fukuoka and Noto sites were also good representatives for emissions from Japan (51% and 58%, respectively); however, Fukuoka was good for East and North China (12% and 9.3%) and South Korea (20%), and Noto was good for Northeast China (22%) and South Korea (7.1%).

S2 Dry deposition effects

The basic assumption in this analysis is that the BC concentration does not show a significant decrease due to dry deposition during transport from the main source region. Similar to Kanaya et al. (2016), we investigated the effect of dry deposition on BC particles from the main source regions to the receptor sites. Figure S3 is an example of a scatter plot between the $\Delta BC/\Delta CO$ ratio and traveling time at the Noto site, with the mean value of each five-hour bin less than 72 hours. The slope of the exponential best fit line is very low as $1.32 \pm 1.88 \times 10^{-3} \text{ hour}^{-1}$ (mean \pm 95% confidence interval) which is correspondence to 0.02 cm s^{-1} for the mean and 0.06 cm s^{-1} for the upper 95% confidence interval of dry deposition velocities when the mean mixing height was 646 m, as calculated by the HYSPLIT model. Not only the Noto site but also the other three sites also showed low dry deposition velocities within a range between 0.01 and 0.03 cm s^{-1} , suggesting that the assumption is valid.

S3 The variation in the $\Delta BC/\Delta CO$ ratio depends on the residence time

Since the $\Delta BC/\Delta CO$ ratio could be influenced by the residence time over the emission source regions, it should be investigated whether the variation in the $\Delta BC/\Delta CO$ ratio depends on the residence time in the same dominant emission region. Figure S4 shows the mean ratio with the standard deviation (vertical solid lines) divided by 20% intervals of the residence time fraction (total 73 hours) of the dominant emission region, along with a bar plot, which indicates the number of data for each bin. The open square symbols with a vertical dashed line indicate that the number of data was less than five (the 25th percentile of the number of data in each bin). We found that $\Delta BC/\Delta CO$ did not vary significantly according to the fraction of residence time when the number of data (N) was higher than five. The difference between each fraction in the same dominant emission region was statistically insignificant ($p > 0.05$), except for ‘South Korea’ in Fukuoka and ‘Others’ in Noto, when Welch’s t-test and the analysis of variance (ANOVA) were applied to two and more than two groups, respectively. This result indicated that the variation in the $\Delta BC/\Delta CO$ ratio according to the fraction (residence time) could be negligible when N exceeds five for the fraction of the residence time. Hereafter, we used the data that satisfied the threshold ($N > 5$) of each bin for comparison with the REAS emission inventory. To verify whether these results were caused by the influences of other emission regions, the dominant emission region was constrained by considering only direct influences without passing through other emission regions. Although the constrained $\Delta BC/\Delta CO$ ratios were only available for Korea and Japan, the mean ratios did not show a significant difference from the original ratio, implying that the effects of other emission regions were not significant.

S4 Uncertainty of regional and seasonal $\Delta BC/\Delta CO$ ratios

The $\Delta BC/\Delta CO$ ratio could be influenced by applying difference estimation methods for the CO baseline and altitude criteria for allocation of the dominant emission region. First, there are several ways to determine the CO baseline, mainly depending on the measurement period. For intensive measurement periods, the CO baseline can be calculated from the 5th percentile of data (Matsui et al. 2011; Miyakawa et al., 2017) or the x-intercept of the best-fit line between BC and CO (Oshima et al., 2012). It can also be calculated by the 5th percentile of the CO concentration from monthly (Verma et al. 2011) or moving 14-day (Kanaya et al. 2016) from long-term measurements. We tested the difference in CO baselines calculated from the 5th

percentile of the moving 14-day (our method) and monthly CO data (Figure S5). The difference in the CO baseline from the monthly data was slightly lower (-2 ppbv; -1.9%) than our estimation. Moreover, the mean $\Delta BC/\Delta CO$ ratios from the two different methods did not show significant differences ($5.82 \text{ ng m}^{-3} \text{ ppb}^{-1}$ for our estimation and $5.87 \text{ ng m}^{-3} \text{ ppb}^{-1}$ for monthly data), when Welch's t-test was applied ($p > 0.1$). Second, we also checked the difference in $\Delta BC/\Delta CO$ which can be caused by applying 1.5 km as a threshold to determine the dominant emission region. There was no significant difference in the regional $\Delta BC/\Delta CO$ ratios between 2.5 and 1.5 km when Welch's t-test was applied ($p \geq 0.1$). For the seasonal variation, though five cases (spring, fall and winter in East China, fall in North China and winter in Northeast China) of recalculated REAS BC/CO values showed significant differences ($p < 0.05$), the ratios of those cases varied within $\pm 1.4 \text{ ng m}^{-3} \text{ ppb}^{-1}$ ($\pm 15\%$), indicating that the MFBs were preserved. From these results, we confirmed the representativeness of our regional and seasonal $\Delta BC/\Delta CO$ analysis.

S5 Footprint for Northeast China

Although the backward trajectory for Gosan passed a similar region to that for Baengnyeong (Figure S7) and the difference in the $\Delta BC/\Delta CO$ ratio due to residence time was negligible, it was hard to exclude the possibility of mixing with emissions from South Korea from the beginning. The high $\Delta BC/\Delta CO$ in the low-residence time fraction for Northeast China in Gosan also supported the possibility of influence from South Korea (Figure S4).

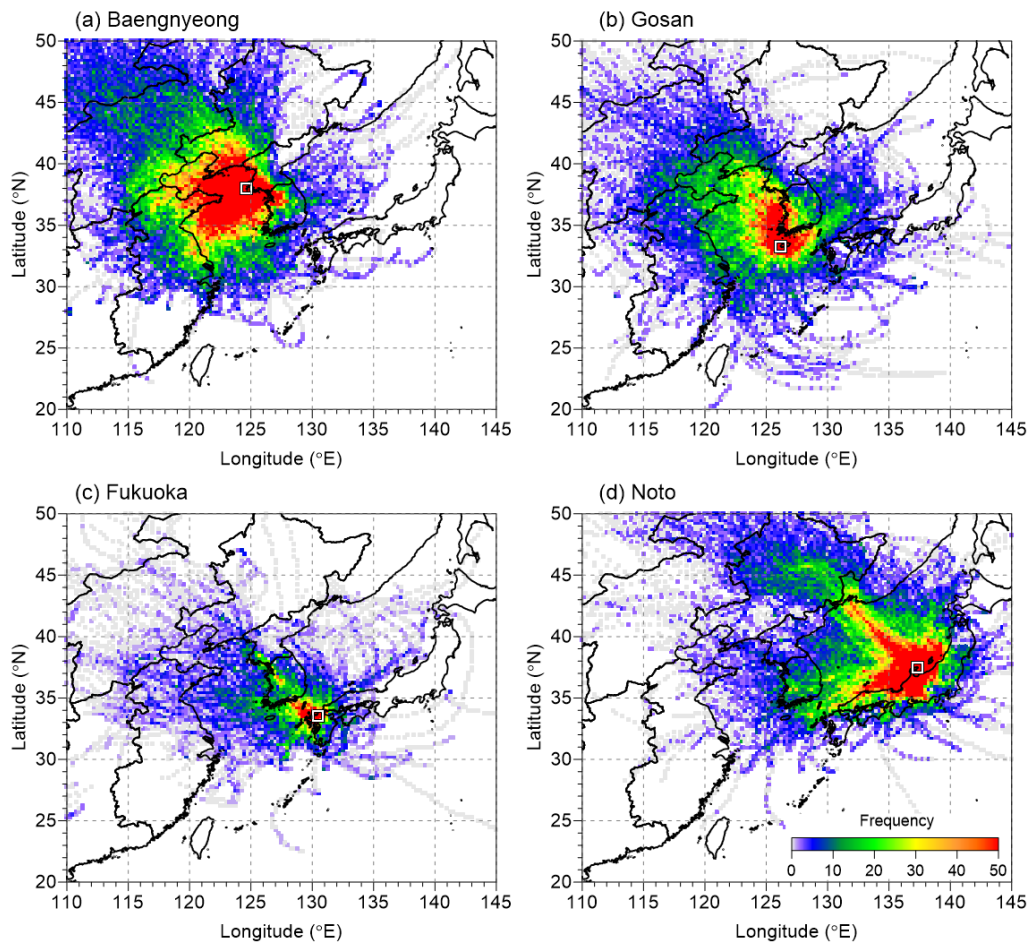


Figure S1. Footprint of the total number of backward trajectory endpoints for a $0.5^{\circ} \times 0.5^{\circ}$ grid cell depending on the measurement site.

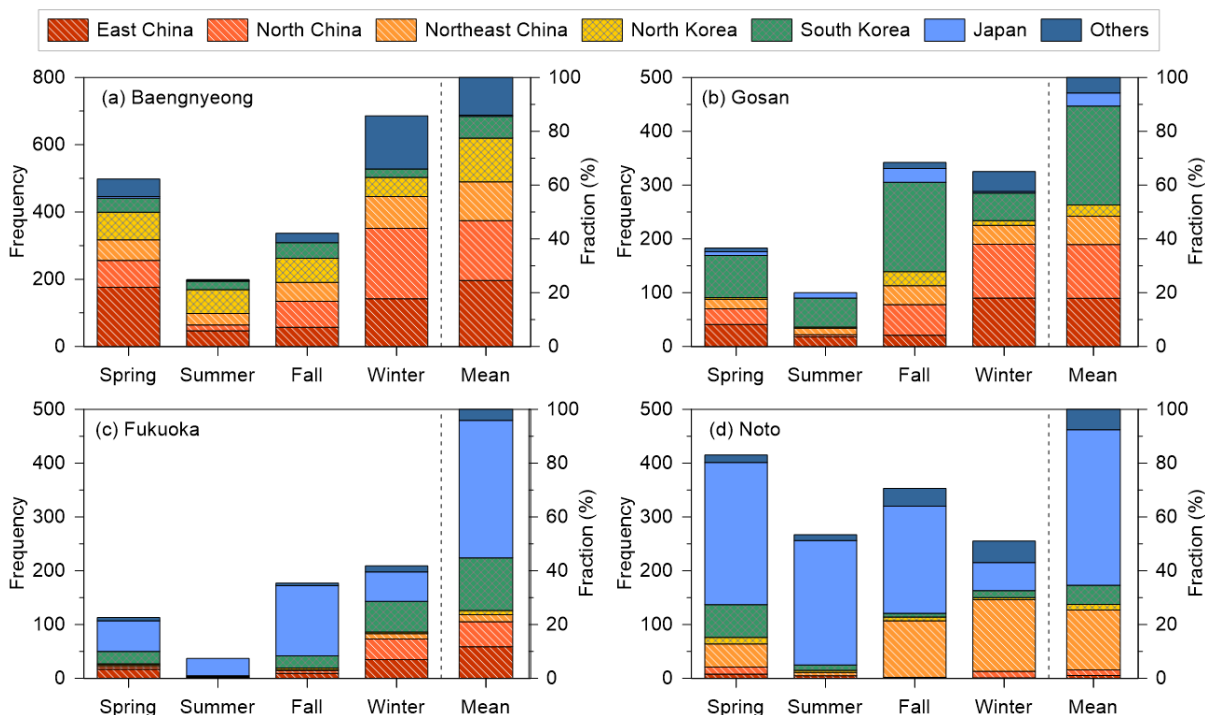


Figure S2. Seasonal variation in the frequency (left side of the dashed lines) and fraction (right side of the dashed lines) for backward trajectory-passed areas (dominant emission regions) in (a) Baengnyeong, (b) Gosan, (c) Fukuoka and (d) Noto.

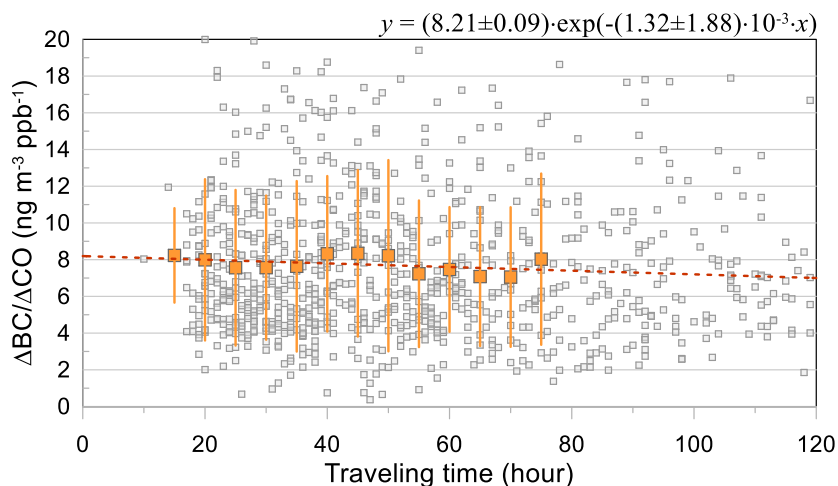


Figure S3. Scatter plot between the $\Delta BC/\Delta CO$ ratio and traveling time in Noto when the APT was zero. The gray squares indicate every observed data point, and orange squares with vertical lines represent the means and standard deviations of five-hour bins for less than 72 hours. The dashed line indicates the best-fit line.

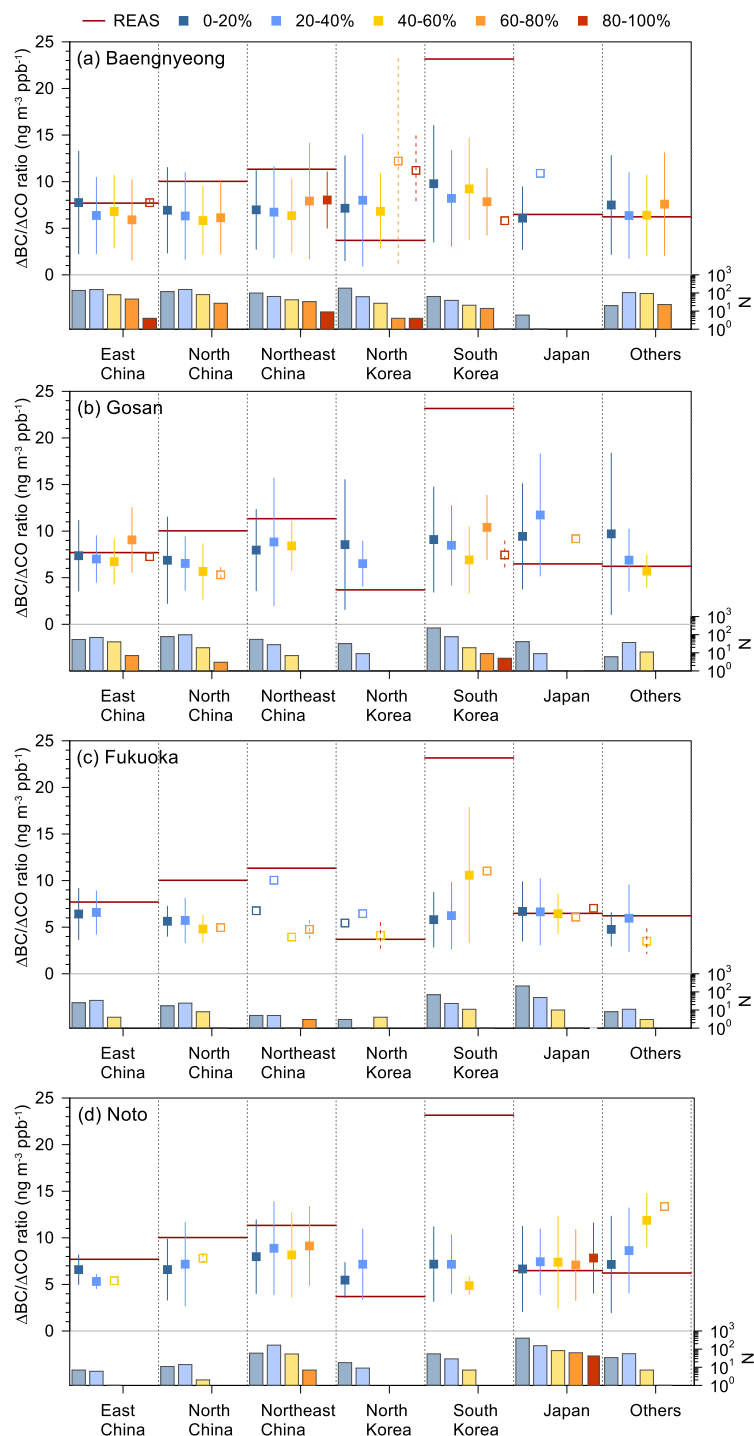


Figure S4. The measured $\Delta BC/\Delta CO$ ratios at four measurement sites depending on the residence time fraction in the dominant emission region. The colored symbols with solid lines and the open symbols with dashed lines indicate the mean and standard deviation of each bin for numbers of data ($N > 5$ and $N \leq 5$, respectively). The bar graphs on the bottom indicate the number of data in each bin and the dominant region. The horizontal red lines depict BC/CO ratios from the REAS emission inventory.

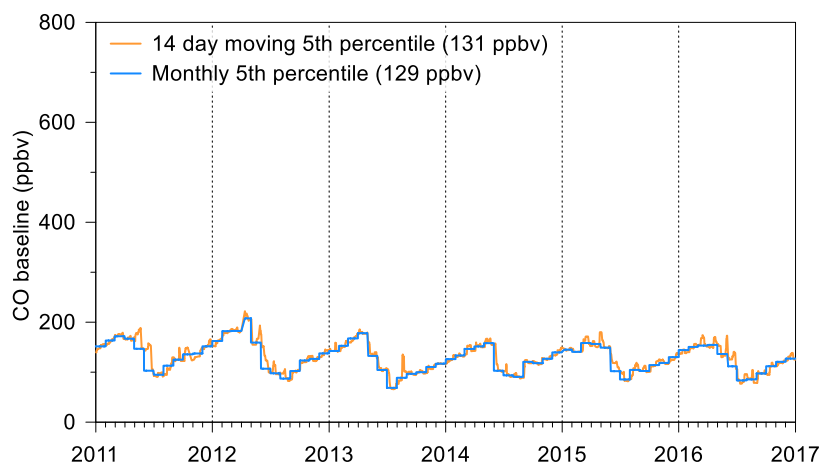


Figure S5. Time series of CO baselines calculated by different methods (14-day moving 5th and monthly 5th percentiles) at Noto.

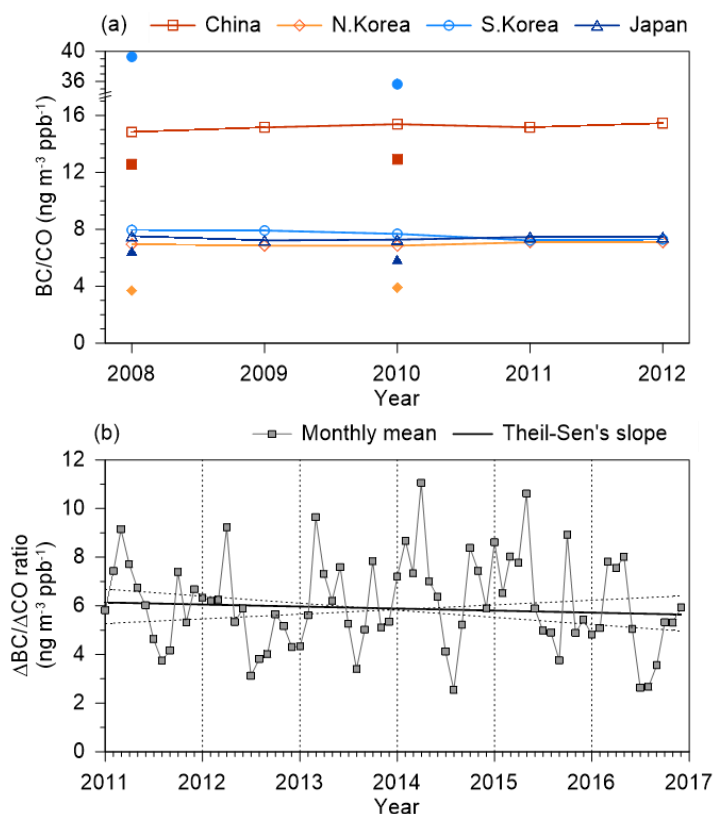


Figure S6. (a) Time series of the BC/CO ratios from the Emissions Database for Global Atmospheric Research (EDGAR v4.3.2; open symbols) during 2008 – 2012 and MIX emission inventory (filled symbols) in 2008 and 2010. (b) Time series of the monthly means of the $\Delta\text{BC}/\Delta\text{CO}$ ratio with Theil-Sen's slope during the measurement periods at Noto. The Theil-Sen's slope of the $\Delta\text{BC}/\Delta\text{CO}$ ratio indicated a slight decreasing trend of the $\Delta\text{BC}/\Delta\text{CO}$ ratio at $-0.08/\text{year}$; but the trend was statistically insignificant ($p > 0.1$). Insignificant trends of the $\Delta\text{BC}/\Delta\text{CO}$ ratio were also observed at the other sites.

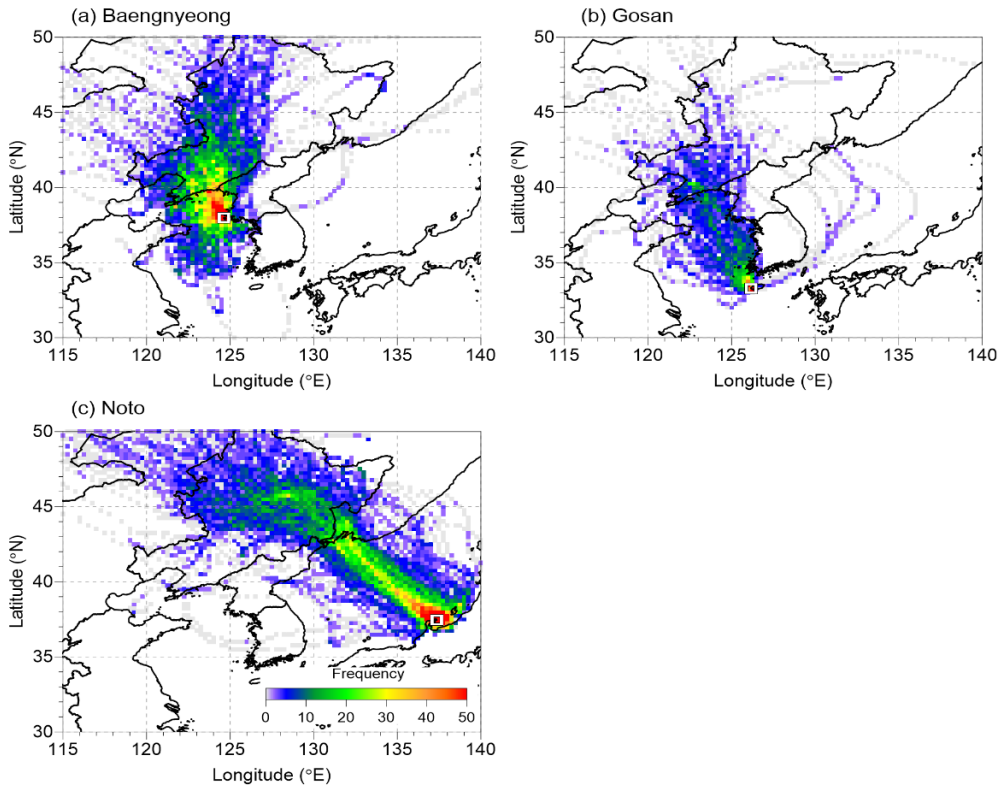


Figure S7. Same as Figure S1, except for the backward trajectory from Northeast China.

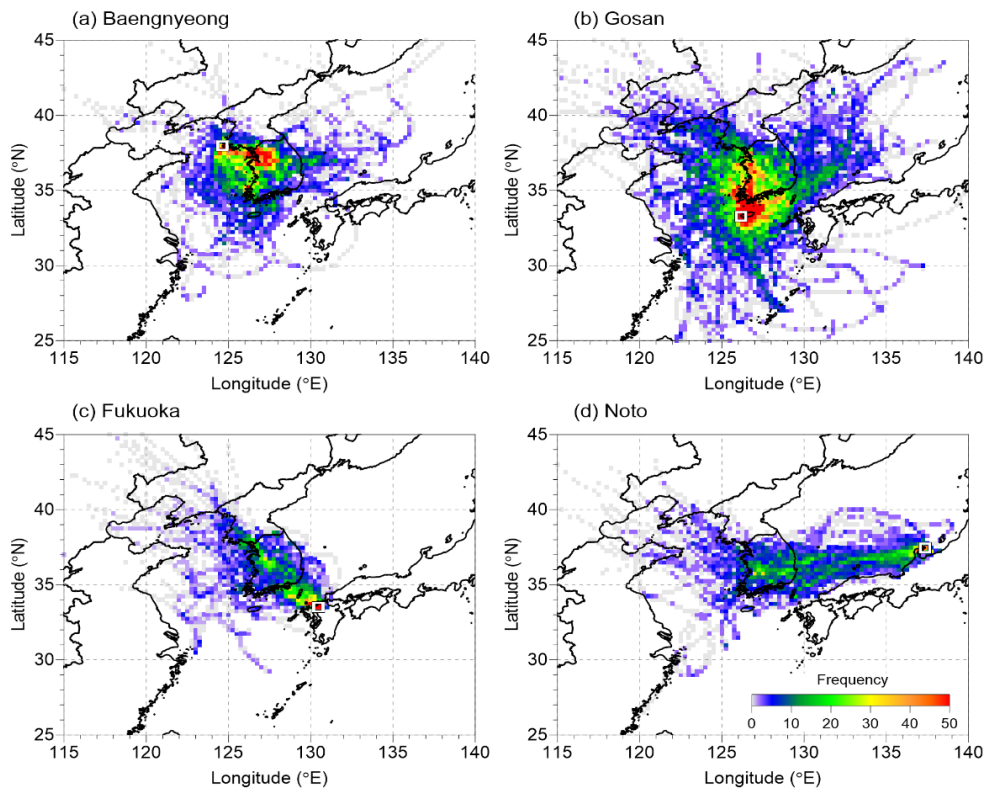


Figure S8. Same as Figure S1, except for the backward trajectory from South Korea.

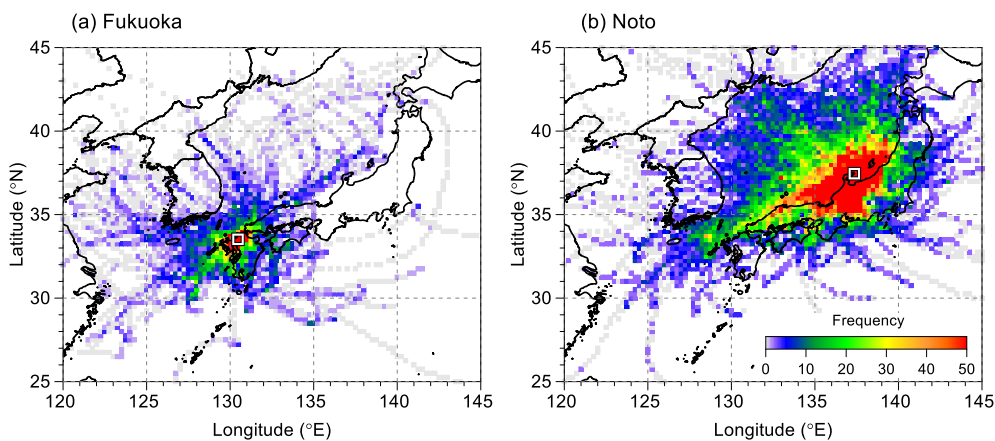


Figure S9. Same as Figure S1, except for the backward trajectory from Japan.

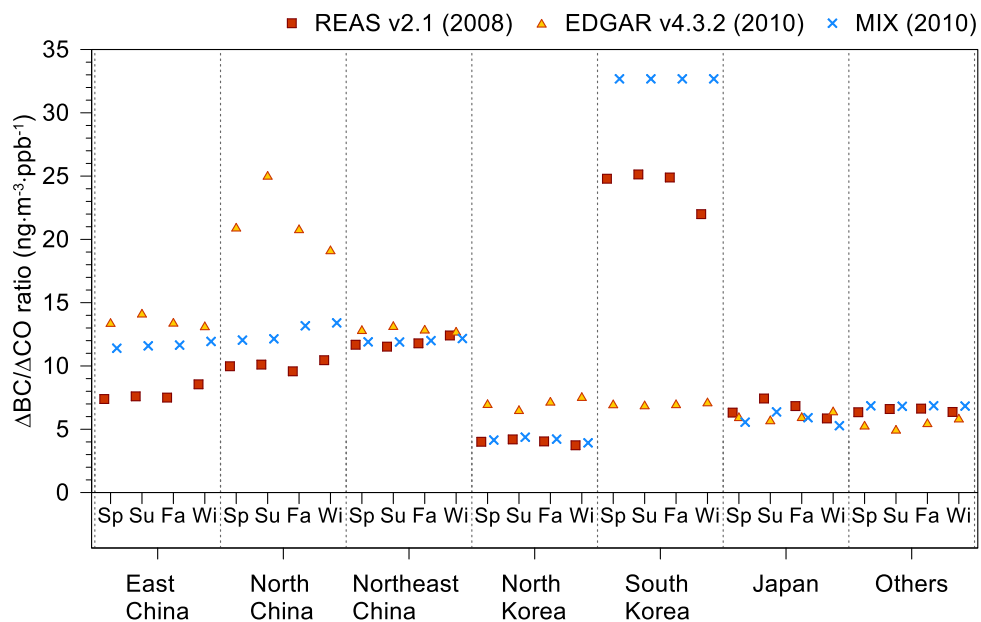


Figure S10. Seasonal variations of the overall regional mean BC/CO ratio according to different bottom-up emission inventories. The number in parentheses in each inventory indicates the base year. The abbreviation of ‘Sp’ to ‘Wi’ indicates spring to winter.